MICROSCOPIC TEXTURE COMPONENTS CLASSIFICATION FOR IMAGE SEGMENTATION

*Eva Hoštálková, Aleš Procházka, Martina Mudrová, and Alena Michalcová**

Department of Computing and Control Engineering, *Department of Metals and Corrosion Engineering
Institute of Chemical Technology, Prague
Technicka 5, 160 00 Prague 6, Czech Republic
phone: + 420 220 444 198, web: http://dsp.vscht.cz/
email: Eva.Hostalkova@vscht.cz, A.Prochazka@ieee.org, Martina.Mudrova@vscht.cz, Alena.Michalcova@vscht.cz

ABSTRACT

The paper presents the possibility of using a sliding window for image feature extraction in order to identify image regions of interest. The study includes the comparison of feature extraction methods both in the space and frequency domains using the discrete Fourier transform and the discrete wavelet transform to achieve reliable classification results for a given application. The compactness of feature clusters is evaluated exploiting a proposed numerical criterion. In case of real image data, the clusters compactness can often be improved by employing a chosen smoothing method on the raw data. In this paper, the procedure of smoothing, feature extraction and classification is applied to microscopic images of aluminum alloys in order to isolate regions of similar properties and to study their relationship. To achieve this goal the sliding window classification results are combined and isolated misclassified subregions repaired. The proportion of misclassified regions is then used for the evaluation of the efficiency of the proposed method along with the proposed measure of cluster compactness.

1. INTRODUCTION

Automated detection of image areas of different structures represents a problem being solved in many engineering, technological and biomedical applications [13, 14, 16, 3]. In the field of microscopic imagery, it is often necessary to employ methods which are invariant to scale, rotation, translation or illumination [20, 19, 8].

The motivation of this paper is automated classification of image structures in microscopic images of metal alloys.

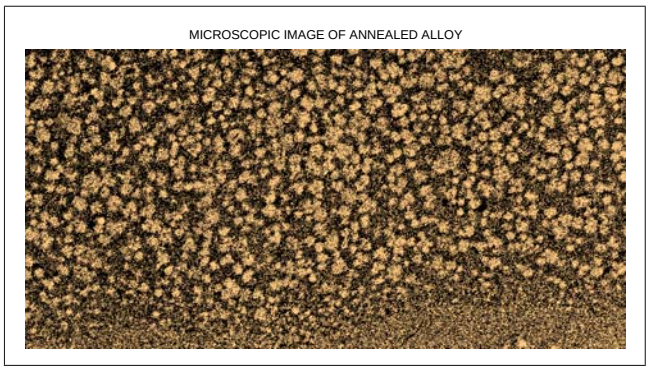

Figure 1: Microscopic image of an aluminium alloy sample with areas of different textures caused by annealing

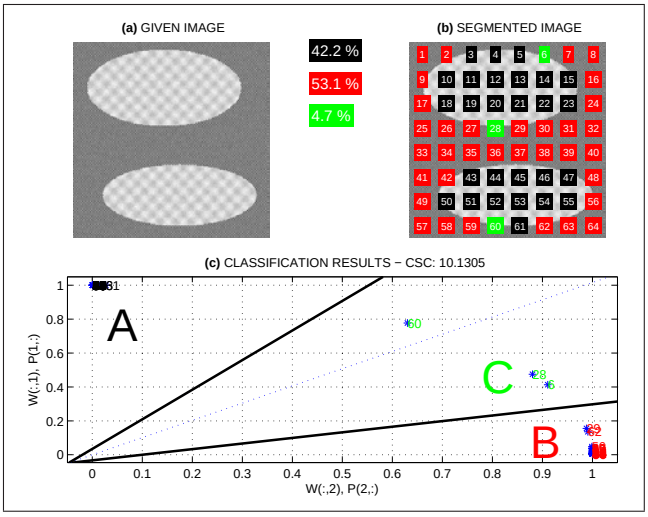

Figure 2: Segmentation of a simulated image presenting **(a)** the original image, **(b)** the result of individual subimages classification, and **(c)** visualization of the features computed by the discrete wavelet transform

Aluminium alloys are widely used in the car and aero industries for its favorable physical properties, such as low density. One of the usage limitations is insufficient temperature resistance (up to 200 °C). This problem forms a specific research topic of a project solved at the Institute of Chemical Technology in Prague. The project is devoted to finding the optimal admixture of cerium (Ce) into an Al-Cr-Fe-Ti-Ce alloy obtained by fast cooling so as to sustain temperatures up to 400 °C. To investigate the improved temperature stability, alloys of different content of cerium are annealed over a certain period of time and the resulting quality changes of the originally homogeneous structures are observed with an electronic microscope producing images such as in Fig. 1. The aim of the work is to detect the homogeneous and the coarser-texture areas by the means of image processing in order to evaluate the amount of temperature degradation.

A simulated image approximating this problem is presented in Fig. 2(a). A possible approach presented in this paper is based upon the sliding window used for feature extraction from individual subimages and subsequent feature classification using the artificial neural networks. This process is presented in Figs 2(b) and (c), where a pair of image features computed by the discrete wavelet transform (DWT) and the result of classification are visualized.

Mathematical methods associated with the process of image classification [18] include methods of image analysis and de-noising [1, 12, 9, 21] followed by feature extraction [15] either in the space, frequency, or wavelet domains [11, 2, 6, 4]. Accordingly, this paper compares the classification results achieved by neural networks [10, 5] using these different methods of feature extraction. As a quality measure of feature clusters, we propose the use of a new criteria function [17] described further.

The proposed algorithm is applied both to simulated images and real microscopic images presenting the efficiency of the suggested method.

2. TEXTURE FEATURE EXTRACTION

Appropriate selection of a feature extraction method forms a crucial point in obtaining as compact clusters as possible for efficient classification.

The study has been devoted to the selection of $R=2$ features for each subimage $\{I_k\}_{k=0}^{Q-1}$ only forming the two row pattern matrix $\mathbf{P}_{R,Q}$ for better visualization even though more features can provide better basis for their classification.

2.1 Space-Domain Features

Two types of space-domain features representing the median and the standard deviation, $f_{k,1}^{(s)}$ and $f_{k,2}^{(s)}$, resp., were used for the individual subimages $\{I_k\}_{k=0}^{Q-1}$ of the size $M\times N$ given as

$$f_{k,1}^{(s)} = median\{I_k(m,n)\} \quad (1)$$

$$f_{k,2}^{(s)} = \frac{1}{M\,N}\sqrt{\sum_{m=0}^{M-1}\sum_{n=0}^{N-1}(I_k(m,n)-\overline{I_k})^2} \quad (2)$$

where $\overline{I_k}$ stands for the mean value of the k-th subimage. Difference images were used for numerical experiments as well.

2.2 Frequency-Domain Features

Another set of features has been computed in the frequency domain using the discrete Fourier transform (DFT) of each subimage I_k

$$\widehat{I_k}(\omega_1,\omega_2) = \sum_{m=0}^{M-1}\sum_{n=0}^{N-1} I_k(m,n)e^{-j\,\omega_1 n}e^{-j\,\omega_2 m} \quad (3)$$

The features $f_{k,1}^{(f)}$ and $f_{k,2}^{(f)}$ have been computed as the means of the magnitudes of $\widehat{I_k}$ in selected two-dimensional frequency bands.

2.3 Space-Scale Features

The space-scale features have been computed by the discrete wavelet transform (DWT) employing selected wavelet filters in a multi-level decomposition process.

Each level of image decomposition is separable into one-dimensional (1D) processing of the rows and subsequent transformation of the result column-wise. For each new level $j+1$, the scaling coefficients $\mathbf{c}_{j+1}^{L}$ (or the wavelet coefficients $\mathbf{c}_{j+1}^{H}$) of length V are produced via convolution of the scaling coefficients $\mathbf{c}_{j}^{L}$ from the previous level j with the low-pass filter h_0 (or high-pass filter h_1) of U taps and downsampling by coefficient 2

$$c_{j+1}^{L}(v) = \sum_{u=0}^{U-1} h_0(u)\,c_j^L(2v-u) \quad (4)$$

$$c_{j+1}^{H}(v) = \sum_{u=0}^{U-1} h_1(u)\,c_j^L(2v-u) \quad (5)$$

where $v=0,1,\ldots,V-1$, $j=0,1,2$, and $\mathbf{c}_0^L$ represents the original signal. The results of row-wise DWT $\mathbf{c}_{j+1}^{L}$ and $\mathbf{c}_{j+1}^{H}$ are then transformed column-wise to obtain four sets of 2D DWT coefficients $\mathbf{c}_{j+1}^{LL}$, $\mathbf{c}_{j+1}^{LH}$, $\mathbf{c}_{j+1}^{HL}$, and $\mathbf{c}_{j+1}^{HH}$. After the wavelet decomposition of each subimage I_k the median value of squared wavelet coefficients of selected scales have been used to estimate features $f_{k,1}^{(w)}$ and $f_{k,1}^{(w)}$ for each subimage.

3. IMAGE SMOOTHING

To improve the classification results the median filtering or wavelet shrinkage has been used for image smoothing. The wavelet shrinkage algorithm consists of decomposition of the image to level 1 using the selected wavelet function. The wavelet coefficients of all three subbands $\mathbf{c}_1^{HH}$, $\mathbf{c}_1^{LH}$, and $\mathbf{c}_1^{HL}$ have then been modified using the soft global thresholding technique. The threshold value has been estimated as

$$\delta^{(s)} = \sqrt{2\,\sigma_n^2\,\log L} \quad (6)$$

where L is the number of wavelet coefficients to be thresholded and σ_n is the standard deviation of additive noise possibly estimated as the MAD (Median Absolute Deviation) given as

$$\sigma_n = median\{\,|\,\mathbf{c}_1^{HH}\,|\,\}/0.6745 \quad (7)$$

where the constant in the denominator corresponds to the normal distribution. This robust estimation technique assumes the $\mathbf{c}_1^{HH}$ subband containing the highest frequencies to be dominated by noise.

4. CLASSIFICATION

Fig. 3 compares the classification results for the simulated image using the space-domain features with those obtained via the DFT. The results differ especially at the regions boundaries.

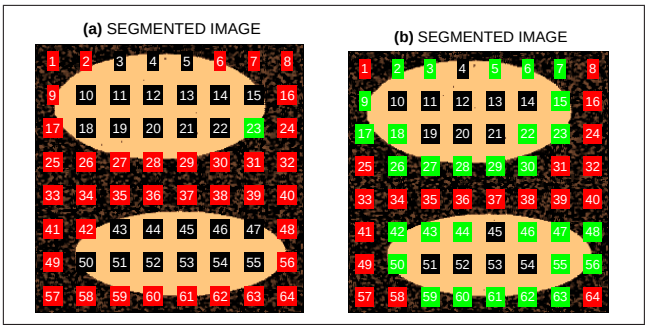

Figure 3: Comparison of the simulated image classification using **(a)** the space-domain features ($CSC=0.537$) and **(b)** the frequency-domain features ($CSC=0.551$) after median filtering

During the segmentation process, each subimage confined by the sliding window is represented by R features which are organized in the pattern matrix $\mathbf{P}_{R,Q}$ and form clusters in the R-dimensional space. The proposed classification algorithm is based upon the application of the self-organizing neural networks [10, 7] using Q feature vectors as patterns for the input layer of the neural network. The number S of the output layer elements is equal to the number of classes. During the learning process, the network weights are changed to minimize the distances between each input vector and the corresponding weights of the winning neuron characterized by its coefficients closest to the current pattern. In case that the process is successfully completed, the network weights belonging to separate output elements represent typical class individuals.

The complete algorithm includes the following steps:

1. Estimation of feature vectors for all subimages to form feature matrix
2. Initialization of network weights and the learning process coefficients
3. Iterative application of the competitive process and Kohonen learning rule for all feature vectors during the learning stage
4. Simulation to find class assignment of individual feature vectors

To compare the classification results of Q signal segments with the feature matrix $\mathbf{P}_{R,Q} = [\mathbf{p}_1, \mathbf{p}_2, \ldots, \mathbf{p}_Q]$ for a selection of different sets of $R = 2$ features and C classes a specific criterion [17] has been designed. Each class $i = 1, \ldots, C$ is characterized by the mean distance of the column feature vectors $\mathbf{p}_{j_k}$ belonging to the class segments j_k for indices $k = 1, 2, \ldots, N_i$ from the class center in the $i-$th row of the matrix $\mathbf{W}_{C,R} = [\mathbf{w}_1, \mathbf{w}_2, \ldots, \mathbf{w}_C]'$ by relation

$$ClassDist(i) = \frac{1}{N_i} \sum_{k=1}^{N_i} dist(\mathbf{p}_{j_k}, \mathbf{w}_i) \qquad (8)$$

where N_i represents the number of segments belonging to class i and the function $dist$ evaluates the Euclidean distance of two vectors. The classification results can then be numerically characterized by the mean value of average class distances related to the mean value of the class centers distances obtained through the learning process and described as

$$CSC = mean(ClassDist)/mean(dist(\mathbf{W}, \mathbf{W}')) \qquad (9)$$

This Cluster Segmentation Criterion (CSC) produces low values for compact and well separated clusters while closely spaced clusters with extensive dispersion result in high CSC values.

The numerical results for different feature extraction methods producing $R=2$ feature sets each are summarized in Tab. 1 of CSC values for different images. It is possible to conclude that all used types of classification parameters provide similar results, however, the wavelet features perform slightly better for all images. As displayed in Fig. 4, visual evaluation of the percentage of misclassified image segments at region boundaries indicates the suitability of this method.

Table 1: CLUSTER COMPACTNESS EVALUATION FOR DIFFERENT FEATURE EXTRACTION METHODS AND CLASSIFICATION INTO 3 CLASSES WITHOUT IMAGE DE-NOISING

Feature extraction method	*Simulated Image*	*Real Image 1*	*Real Image 2*
Space domain - CSC:	0.537	0.727	0.637
Frequency domain - CSC:	0.551	0.605	0.599
Wavelet domain - CSC:	0.441	0.453	0.531

5. RESULTS

The selected results of real data processing are presented in Fig. 4 showing classification for non-overlapping windows and features obtained by the average frequency components evaluation in given bands obtained by the discrete Fourier transform and average values of discrete wavelet transform in selected scales. Results are affected mostly by selected image preprocessing methods, window size, feature extraction methods and classification algorithms.

The resulting CSC measures averaged over several experiments are presented in Fig. 5 indicating that the frequency and the wavelet domain features mostly surpass the space domain features.

6. CONCLUSION

The paper presents selected methods of microscopic images analysis for automated region detection. The processed images of aluminium alloys reveal areas of structural changes of the originally homogeneous texture as a consequence of the annealing process. The size of these areas characterizes the alloy quality. Prior to application of image segmentation methods, it proved necessary to preprocess the image data by smoothing and histogram alteration.

The proposed region detection algorithm is based upon feature extraction using the sliding window and subsequent

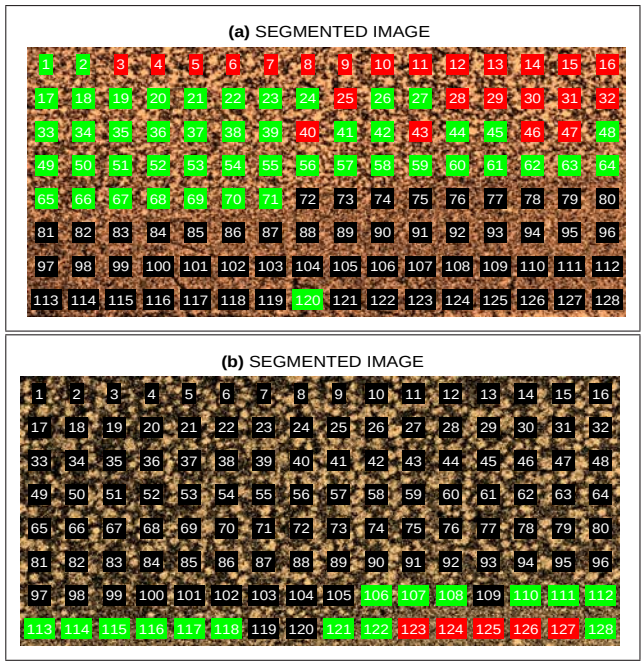

Figure 4: Segmentation results for two different alloy samples using **(a)** the space-domain features extracted from the real image 2 smoothed by wavelet shrinkage ($CSC = 0.574$) and **(b)** the DWT-based features from the real image 1 depicted in Fig. 1 ($CSC = 0.558$)

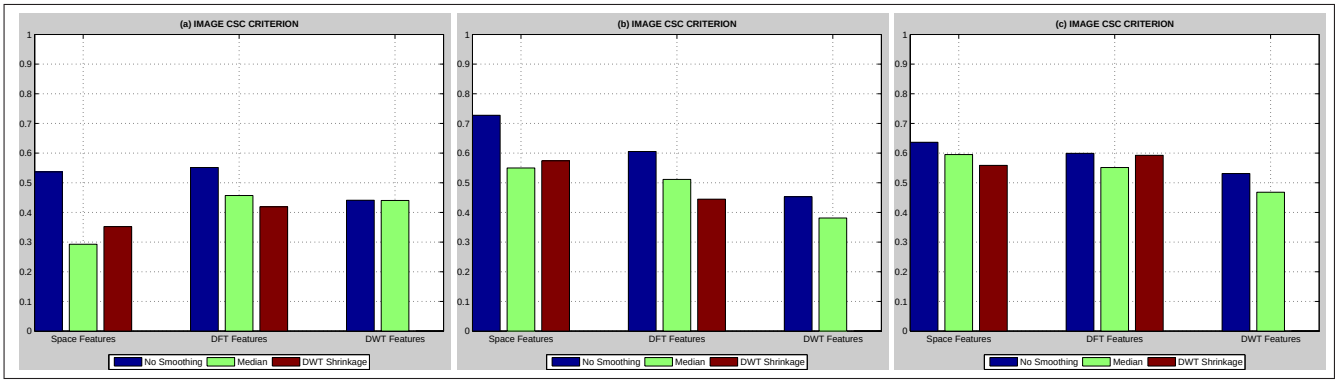

Figure 5: Classification results using different smoothing and image classification methods displaying the CSC criterion values for **(a)** the simulated image from Fig. 2(a), **(b)** the real image 1 from Fig. 1, and **(c)** the real image 2 from Fig. 4(a)

classification using an artificial neural network. Considering the data properties, we produce three different feature computation methods based on the space domain, the Fourier domain, and the wavelet domain. According to the CSC measure of clusters quality, the wavelet domain features slightly surpass the other methods.

Further work will be devoted to the application of overlapping windows for more detail classification and to the search for the most efficient kind of features and their combination to produce compact and well separated clusters. Another aim of the work will include the evaluation of the percentage of successfully classified segments for larger number of experiments.

Acknowledgments

The work has been supported by the grant of the Faculty of Chemical Engineering of the Institute of Chemical Technology, Prague No. MSM 6046137306 and KAN 300100801.

REFERENCES

[1] A. Kadyrov and M. Petrou. The trace transform and its applications. *IEEE Transactions on Pattern Analysis and Machine Intelligence*, 23:811–828, 2001.

[2] A. P. Bradley. Shift-invariance in the Discrete Wavelet Transform. In *Proceedings of VIIth Digital Image Computing, Sydney*. IEEE, 2003.

[3] A. Procházka and J. Ptáček. Wavelet Transform Application in Biomedical Image Recovery and Enhancement. In *The 8th Multi-Conference Systemics, Cybernetics and Informatic, Orlando, USA*, volume 6, pages 82–87. IEEE, 2004.

[4] S. Arivazhagan and L. Ganesan. Texture Segmentation Using Wavelet Transform. *Pattern Recogn. Lett.*, 24(16):3197–3203, 2003.

[5] C. M. Bishop. *Neural Networks for Pattern Recognition*. Oxford University Press, 1995.

[6] R. N. Bracewell. *Fourier Analysis and Imaging*. Kluwer Academic Press, 2003.

[7] D. I. Choi and S. H. Park. Self-Creating and Organizing Neural Networks. *IEEE Trans. Neural Networks*, 5(4):561–575, July 1994.

[8] David G. Lowe. Object Recognition from Local Scale-Invariant Features . In *Proceedings of the International Conference on Computer Vision, Corfu*. IEEE, 1999.

[9] R. C. Gonzales, R. E. Woods, and S. L. Eddins. *Digital Image Processing Using MATLAB*. Prentice Hall, 2004.

[10] S. Haykin. *Neural Networks, A Comprehensive Foundation*. Macmillan College Publishing Company, New York, 1994.

[11] I. W. Selesnick and R. G. Baraniuk and N. G. Kingsbury. The Dual-Tree Complex Wavelet Transform. *IEEE Signal Processing Magazine*, 22:123–151, 2005.

[12] J. L. Starck and E. Candes and D.L. Donoho. The Curvelet Transform for Image Denoising. *IEEE Trans. on Image processing*, 11(6):670–684, 2002.

[13] K. Jafari-Khouzani and H. Soltanian-Zadeh. Rotation-invariant multiresolution texture analysis using Radon and wavelet transforms. *IEEE Transaction on Image Processing*, 14(6):783–795, 2005.

[14] Chin-Yung Lin, Min Wu, J. A. Bloom, I. J. Cox, M. L. Miler, and Yui Man Lui. Rotation, Scale, and Translation Resilient Watermarking for Images. *IEEE Transaction on Image Processing*, 10(5):767–782, 2001.

[15] M. Nixon and A. Aguado. *Feature Extraction & Image Processing*. NewNes Elsevier, 2004.

[16] A. Procházka, A. Gavlasová, and K. Volka. Wavelet Transform in Image Recognition. In *International conference ELMAR05, Zadar. Croatia*. IEEE, 2005.

[17] A. Procházka, E. Hošťálková, and A. Gavlasová. Wavelet Transform in Image Regions Classification. In *Proceedings of the 8th IMA Conference on Mathematics in Signal Processing*, pages 34–38. The Institute of Mathematics and its Applications, U.K., 2008.

[18] C. W. Shaffrey. *Multiscale Techniques for Image Segmentation, Classification and Retrieval*. PhD thesis, University of Cambridge, Dept of Engineering, 2003.

[19] Simon M. Stringer. Invariant Object Recognition in the Visual System with Novel Views of 3D Objects. *Neural Computing*, (14):2585–2596, 2002.

[20] L. A. Torres-Mendez, J. C. Ruiz-Suarez, L. E. Sucar, and G. Gomez. Translation, Rotation and Scale-Invariant Object Recognition. *IEEE Transaction on System, Man and Cybernetics*, 30(1):125–130, 2000.

[21] Saeed V. Vaseghi. *Advanced Digital Signal Processing and Noise Reduction*. Wiley & Teubner, West Sussex, U.K., second edition, 2000.